mindray
healthcare within reach

M-Reference

Technical White Paper

Li Shuangshuang, Lan Bangxin, Li Jinyang, Xu Shuming
Ultrasound Imaging System Development Department, Mindray

Contents

M-Reference

Multi-Parameter Ultrasound Imaging and Analysis

A Novel Solution for Ultrasound Imaging

Li Shuangshuang, Lan Bangxin, Li Jinyang, Xu Shuming

Introduction

In recent years, in vivo non-invasive imaging diagnosis has attracted extensive attention from researchers worldwide. With the continuous development of ultrasound imaging technology, various quantitative imaging technologies have emerged globally. These technologies evaluate pathological tissues from the perspectives of ***mechanical parameters, acoustic parameters, morphological parameters, and blood perfusion parameters***. The goal is to achieve quantitative and specific diagnosis of target tissues non-invasively.

Given the maturity of various quantitative parameters, multi-parametric ultrasound diagnosis has become a research hotspot, a trend, and an expert consensus [1-5].

Among these parameters, strain elastography and acoustic radiation force (ARF) based shear wave elastography are well-established ***mechanical parameters for tissue***, and numerous studies have confirmed the clinical value of ultrasound elastography in various applications [6-13]. It is particularly useful in the auxiliary diagnosis of liver fibrosis, liver cirrhosis, and certain cancers (such as breast cancer, thyroid cancer, cervical cancer, etc.). With the emergences of many large-sample clinical multi-center studies and comparative studies [14-16], ultrasound elastography has become increasingly mature and standardized in clinical practice. Moreover, due to the fact that tissue stiffness changes are generally associated with the progression of many different clinical diseases or tissue injuries, the clinical application of elastography has also expanded to new fields such as muscles, gynecology, obstetrics, medical artificial intelligence, lungs, prostate, and heart [17-23], demonstrating tremendous clinical potential and arousing continuous interest from researchers. As an emerging ***mechanical parameter*** related to tissue inflammation, viscoelastography can be used to study the viscosity and dispersion parameters of tissues [24-26]. In early clinical validations, it has also shown great clinical potential as a supplement to elasticity in the study of tissue's mechanical parameters, attracting widespread attention from researchers worldwide.

The study of the relationship between ***tissue's acoustic parameters, tissue's morphological parameters***, and pathology or tissue status has always been important. With the advancement of ultrasound technology and platforms, the research results are gradually implemented in clinical practice, such as in liver and breast fields. Conventional ultrasound imaging has become widely used due to its non-invasiveness, real-time capability, and low cost. However, it heavily relies on the operator's experience. Based on conventional ultrasound imaging, quantitative ultrasound technologies including ultrasound attenuation, sound speed, and acoustic texture quantitatively evaluate tissue status using radiofrequency echo signals, reducing dependence on operators [27]. Compared to conventional ultrasound images,

quantitative ultrasound based on raw signals not only reduces information loss but also avoids measurement fluctuations introduced by post-processing.

Ultrasound Attenuation analysis technology is an important parameter reflecting the ***acoustic characteristics of tissue***. It reflects the continuous energy loss of ultrasound signals during their propagation in tissues with increasing propagation distance, known as attenuation. In soft tissues, the attenuation of acoustic energy accelerates with increasing depth and frequency, and it is also influenced by the inherent attenuation characteristics of tissues. For example, acoustic energy attenuates faster in fatty liver than normal liver. Another important parameter characterizing the ***acoustic properties of biological tissues*** is the speed of sound. Different tissues exhibit significant differences in the longitudinal wave propagation velocity of ultrasound. Therefore, sound speed technology has attracted attention in clinical research, such as evaluation on liver steatosis and grading of breast masses.

In addition to echo intensity, the observation of tissue differences in conventional ultrasound imaging often relies on echo texture. The spatial distribution of bright and dark speckle, or particles in ultrasound imaging is called texture, which is clinically manifested as speckle size, particle density, etc. In parenchymatous tissues, echo texture is significantly related to the tissue characteristic. For example, as the degree of liver steatosis increases, the attenuation of echoes increases, and the particle size becomes smaller and the particle density becomes denser. Liver texture technology quantifies the ***morphological characteristics*** of liver tissue and reflects the liver steatosis severity.

Contrast-enhanced ultrasound(CEUS) imaging and ultrasound doppler technologies provide ***blood perfusion parameters of tissue***, which can reflect the real-time blood perfusion of tissues. These two technologies have been widely applied in routine examinations and have been proven of huge clinical values in various applications with specific clinical manifestations of tumors. Based on the specific clinical manifestations of the blood supply of tumor tissue, quantitative research tools using these two technologies are expected to achieve non-invasive diagnosis of target tissues [28-29]. Furthermore, with the continuous innovation of ultrasound technology, quantifications based on super resolution CEUS and quantitative analysis of ultra micro angiography (UMA) are expected to achieve more accurate non-invasive diagnosis of lesion tumors by observing and quantifying slow and micro blood vessels.

Real-Time Multi-Parametric Ultrasound Imaging and Analysis Tool

With the deepening of quantitative ultrasound research, tissue changes are reflected in multiple parameters, and single parameters are insufficient to meet clinical needs. Considering sampling errors and operational efficiency, real-time multi-parametric ultrasound imaging and analysis can comprehensively describe tissue status and provide a more comprehensive evaluation and diagnosis.

Mindray's real-time multi-parametric ultrasound imaging and analysis tool (M-Reference) includes Strain Elastography②③, Shear Wave Elastography ① ② ③ , Viscoelastography①②, Liver Texture Index(LTI) ①, UltraSound ATtenuation(USAT) ①, and Target Sound Speed Index(TSSI)①.

① **Liver multi-parametric ultrasound imaging and analysis tool**

② **Breast multi-parametric ultrasound imaging and analysis tool**

These technologies allow real-time research on mechanical parameters, morphological parameters, and acoustic parameters of the liver ①. The obtained parameters include shear wave elastography Young's modulus E (kPa), viscosity coefficient (Pa.s), frequency dispersion (FD) (m/s/kHz), single-frequency shear wave E (kPa), USAT coefficient (dB/cm/MHz), TSSI Cs (m/s), and LTI.

Similarly, real-time research can be conducted on target tissues in the breast② using shear wave elastography, strain elastography, and viscoelastography to study mechanical parameters of tissue. The obtained parameters include shear wave elastography Young's modulus E (kPa), strain, strain ratio (B/A), viscosity coefficient Visco (Pa.s), FD (m/s/kHz), and single-frequency shear wave E (kPa).

Likewise, real-time research can be conducted on target tissues in the thyroid③ using shear wave elastography and strain elastography to study tissue's mechanical parameters. The obtained parameters include shear wave elastography Young's modulus E (kPa), strain, and strain ratio (B/A).

Next, we will provide technical introductions for each function in real-time multi-parametric ultrasound imaging and analysis tool.

Strain Elastography Technology

Ultrasound strain elastography can provide real-time strain images within the region of interest (ROI) and has been widely used in clinical practice for over a decade. It is based on Hooke's law, which states that under the same pressure, hard tissues produce relatively small strain, while soft tissues produce relatively large strain. Therefore, when uniform pressure is applied through the transducer, the strain distribution image of the tissue can reflect the elastic difference between different parts of the tissue. As shown in Figure 1, in simulation, there is a significant difference between the deformation at the target point and uniform surrounding phantom under uniform pressure at the surface.

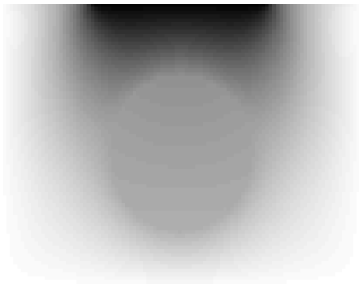

Figure 1: Strain of a simulated phantom

Strain elastography distinguishes the relative stiffness of target tissues from surrounding tissues by identifying the strain produced by tissues under the same pressure. It is a technology for obtaining semi-quantitative/qualitative parameters of target tissues.

Shear Wave Elastography Technology

As shown in Figure 2, the shear wave elastography technology based on ARF can transmit focused ultrasound within the range of medical diagnostic ultrasound power to the tissue using the probe of conventional ultrasound examination. Based on the ARF effect [30,31], the shear wave can be generated in the target region within the tissue. By applying the arrayed emission focus control technology of the Resona platform, a single emission can simultaneously generate a wide range of shear wave sources in the depth range of 0.2 mm to 30 mm. The system then tracks shear wave transmission, and continuously detects and records tissue displacement changes caused by shear wave transmission in the ROI. Finally, through a series of calculations, the transmission velocity of shear waves is obtained, and then parameters such as the elastic modulus of the tissue are deduced [32].

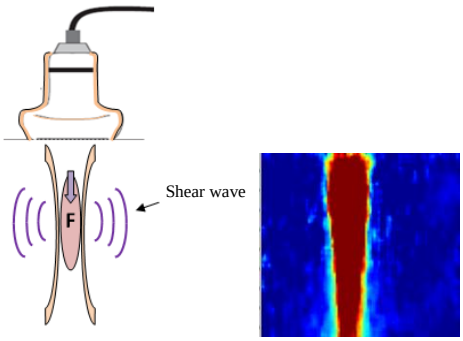

Figure 2: ARF and shear waves

Shear wave elastography mainly displays shear wave transmission velocity or tissue elastic modulus, such as Young's modulus and shear modulus. Young's modulus is the most common indicator of tissue stiffness, and a higher Young's modulus value indicates a higher stiffness. For a linear, elastic, isotropic medium, the Young's modulus is calculated as:

$$E = 3G = 3\rho Cs^2$$

Where, G is the shear modulus; ρ is the density of the tissue; Cs is the transmission velocity of the shear wave. According to the formula, shear waves transmit faster in stiff tissues and slower in soft tissues [33-35].

Shear wave elastography has gained considerable clinical interest by providing quantified tissue hardness measurements. The characteristics of quantitative measurement greatly expand the clinical application of elastography, and also make the development and research of elastography technology reach a new climax.

Viscoelastography Technology

Mindray's viscoelastography is calculated based on shear wave elastography and mainly consists of three steps. The first step is to generate ARF using a transducer to generate shear waves in human body tissue. The second step is to detect the propagation of shear waves in the tissue. In this step, a wide-band shear wave is received. The third step is the calculation of viscoelastography. First, the wide-band shear wave propagation velocity is used to calculate the shear wave elastography. Then, as shown in Figure 3, different frequency components of shear waves in the wide-band shear wave are extracted and their propagation velocities are calculated separately. Finally, using the viscoelasticity fitting model, the viscosity coefficient and FD are calculated for shear wave viscoelastography imaging [36].

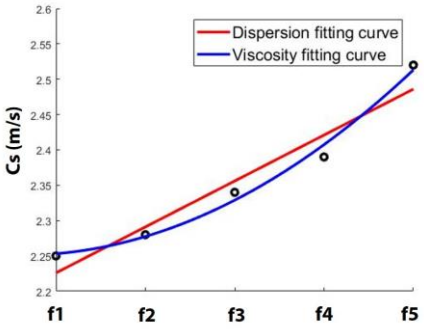

Figure 3: Viscoelasticity fitting curve

In viscoelastography, tissue viscosity is considered. Based on the relationship between shear wave propagation velocity and shear wave frequency, the elastic and viscous measurements of the ROI are obtained and color coded. In early clinical validations, viscoelasticity has shown great clinical potential and a strong correlation with tissue inflammation. It can be used as a supplement to elasticity in the study of tissue mechanical parameters [24-26].

Ultrasound Attenuation Technology

Theoretically, the ultrasound pressure amplitude P propagated for a distance of d in a homogeneous tissue can be approximately represented as $P(d) = P_0 e^{-\alpha f d}$, where P_0 is the initial sound pressure of the signal at $d = 0$, α is the attenuation coefficient (in dB/cm/MHz), f is the frequency (in MHz). For a certain frequency of ultrasound, the intensity of sound energy (in dB) has an approximately linear relationship with the propagation depth (in cm).

The attenuation coefficient of liver tissue generally ranges from 0.4 to 1.0 dB/cm/MHz. In the evaluation of liver steatosis, the higher the degree of fatty liver, the greater the attenuation coefficient, regardless of depth or frequency.

Ultrasound attenuation technologies have been continuously improved through clinical research. For example, in the case of fatty liver, due to the low diagnostic performance of ultrasound technology at early stage and the high cost and low popularity of MRI, there is a great need for a convenient and quantitative tool. Therefore, an ultrasound attenuation parameter called Controlled Attenuation Parameter (CAP) appeared on liver transient elastography devices for fatty liver quantification, which can detect liver steatosis of more than 5% and accurately distinguish between mild and moderate to severe liver steatosis. However, CAP is based on one-dimensional ultrasound signals obtained using a single-element probe and cannot provide visualization of liver structures. It is easily affected by operational error, liver sampling positions, or liver sections, and the repeatability and accuracy of quantitative measurements need to be further improved. Subsequently, Mindray introduced Liver Ultra-Sound Attenuation (LiSA) technology on the Hepatus non-invasive quantitative liver ultrasound instrument, which provides visual image guidance and two-dimensional ultrasound attenuation measurement. It has better sensitivity and specificity in diagnosing liver steatosis grades. However, LiSA technology requires the use of special dedicated probes and cannot provide two-dimensional ultrasound attenuation distribution images, which cannot fully meet research and clinical demand[38]. In recent years, ultrasound attenuation technologies based on conventional ultrasound platforms, such as USAT, Attenuation Imaging (ATI), and Ultrasound-Guided Attenuation Parameter (UGAP), have emerged. They not only have better diagnostic performance but also provide two-dimensional ultrasound attenuation images and quality control tools.

Target Sound Speed Technology

The concept of sound speed, ultrasound propagation speed in tissue, is intuitive and well-known in research. Differences in sound speed between different tissues, such as 1575 m/s in muscles and 1450 m/s in fat, have been discovered early. Some ex vivo liver studies have also shown that higher degree of fatty liver steatosis leads to decreased sound speed. However, due to the complexity of human body structures and the limitations of technological development, traditional medical ultrasound imaging devices usually use fixed sound speed for all kinds of tissue, such as 1540 m/s. In clinical practice, B-mode ultrasound images obtained from different tissues at the same sound speed exhibit significant differences, such as in the liver, breast, and muscles, which is related to the models of conventional beamforming.

With the development of ultrasound technology, clinical research on non-invasive sound speed technologies have gradually started. Mindray introduced the Sound Speed Correct (SSC) function based on the ZST platform, which is a focusing techniques based global sound speed technology that calculates the optimal sound speed based on the beamforming data in the current plane to improve image quality[39]. However, due to the inevitable inclusion of different tissues in the same plane, the application of this sound speed technology in quantitative evaluation is limited. To address this issue, Mindray further introduced spatial coherence based TSSI function, which can measure sound speed within the ROI range based on raw channel data, suppress interference between different tissues, and

demonstrate good performance in phantom validations. This function has shown good prospects in clinical applications of liver and breast.

Liver Texture Index Technology

Ultrasound echo texture is usually considered as the echo amplitude disturbances formed by the scattering of small particles in tissues, thus containing information about the microstructure of tissues. Currently, there are many analysis methods for ultrasound echo texture, among which the most common one is based on the envelope amplitude co-occurrence matrix. Based on the echo signals from spatial positions (i, j), the co-occurrence matrix and then its probability density function $P(i,j|d,\theta)$ can be calculated with the amplitude difference (d) and angular distances (θ). Theoretically, the probability density follows the Rayleigh distribution in a uniform scatter-distributed tissue. It has been found in clinical research that in parenchymatous organs, such as liver parenchyma, the probability density function of ultrasound echoes tends to be closer to the Rayleigh distribution with sever fatty liver, while normal liver significantly deviates from the Rayleigh distribution [40].

Based on ultrasound texture information, Mindray has introduced LTI for liver applications. LTI index represents the deviation between the probability density function of the target tissue and the expected distribution. To quantify liver steatosis, this deviation is normalized to a range of 0 to 4. A smaller value indicates a lighter degree of fatty liver even normal, while a larger value indicates a more severe degree of fatty liver. In prospective studies on fatty liver, LTI has shown good diagnostic performance, especially in terms of sensitivity.

Use of Real-Time Multi-Parametric Ultrasound Imaging and Analysis Tool

Select **M-Ref.Live** on the left side of the screen to start real-time multi-parametric ultrasound imaging and analysis tool. After entering the real-time multi-parametric ultrasound imaging and analysis tool, the pre-acquisition state is on by default. The control panel of multi-parametric ultrasound imaging and analysis tool will appear, including: single mode control panel switch, M-Ref list, layout, acoustic quantification, measurements, interface parameter adjustment, full-screen mode button, settings button and report.

1. Single mode control panel switch: Users can adjust the imaging settings, image display, etc. of the single mode used in multi-parametric ultrasound imaging and analysis tool according to their needs.
2. M-Ref list: The M-Ref list displays the available single mode and optional quantitative parameters.
3. Layout: Users can freely select the real-time imaging or real-time measurement functions that need to be displayed in quad view. As shown in Figure 4, the position of each function window can be adjusted arbitrarily. Each function occupies one window and measurement results and images are displayed after being updated.

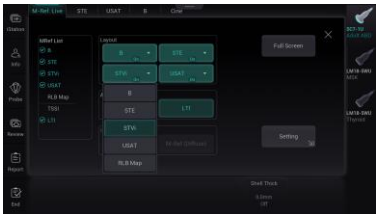

(a)

(b)

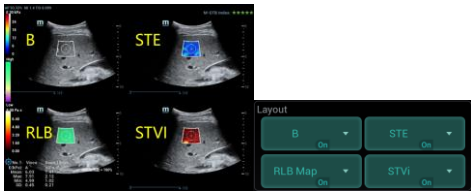

(c)

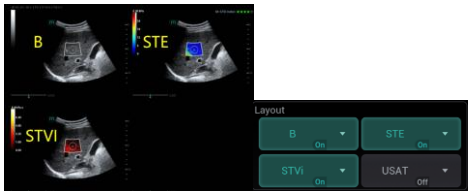

(d)

Figure 4: (a) Control panel interface of real-time multi-parametric ultrasound imaging and analysis tool; (b), (c), (d) Real-time imaging functions selected in Layout.

4. Acoustic quantification: Real-time multi-parametric ultrasound imaging and analysis of liver supports acoustic parameter quantification of TSSI (m/s) and LTI.

5. Measurements: In multi-parametric ultrasound imaging and analysis tool, two quantitative measurement methods are supported: M-Ref(Focal) and M-Ref(Diffuse). M-Ref(Focal) allows measurement using trace, ellipse, or circular measurement boxes. M-Ref(Diffuse) only allows measurement using a circular box.

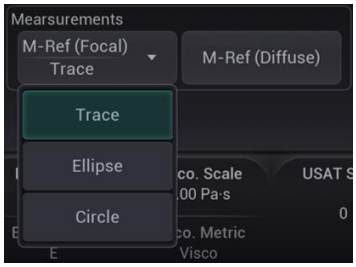

Figure 5: M-Ref(Focal) and M-Ref(Diffuse)

6. Interface parameter adjustment: In the interface parameter area, users can adjust the scale of elastography, scale of viscoelastography, scale of USAT, elastic metric, viscosity metric, and shell size. Other parameters can be adjusted for each single mode after switching to the single mode control panel.

7. Full-screen mode: As shown in Figure 6, the full-screen mode button allows switching between full-screen and non-full-screen display of images.

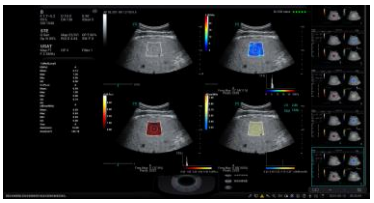

(a)

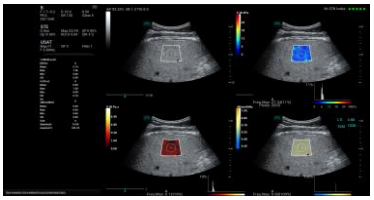

(b)

Figure 6: (a) Non-full-screen display; (b) Full-screen display

8. Settings: As shown in Figure 7, the settings button allows users to select the default quad view layout, whether to start with default acoustic quantification parameters, the display of measurement results using M-Ref(Focal) and M-Ref(Diffuse) measurement methods, whether to enable ratio measurement by selecting "Ratio" and whether to display histograms by switching the Hist option.

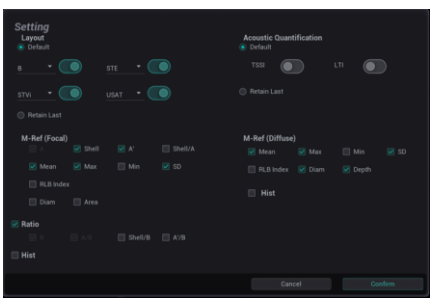

Figure 7: Settings panel

9. Report: After measurement and saving the results using M-Ref(Focal) and M-Ref(Diffuse) measurement methods, the measurement results will be displayed in the report. As shown in Figure 8, M-Ref(Focal) provides more detailed report results for each measurement, while M-Ref(Diffuse) provides a simpler display of measurement results from multiple measurements.

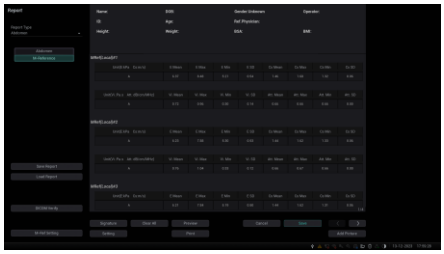

(a)

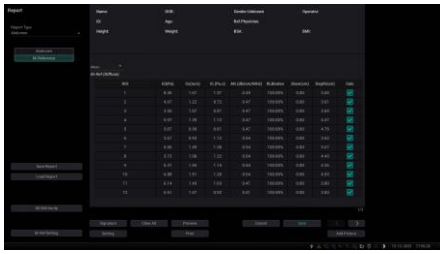

(b)

Figure 8: (a) M-Ref(Focal) measurement report display; (b) M-Ref(Diffuse) measurement report display

"Multi-Parametric Grading Reference" and "Multi-Parametric Grading Radar Chart"

To more intuitively display the measurement results of multi-parametric ultrasound imaging and analysis, Mindray's multi-parametric ultrasound imaging and analysis also provides "Multi-Parametric Grading Reference" and "Multi-Parametric Grading Radar Chart".

By default, the "Multi-Parametric Grading Reference" and "Multi-Parametric Grading Radar Chart" are not displayed in the report. As shown in Figure 9, users need to manually select the staging measurement indicators and values for M-Ref(Focal) or M-Ref(Diffuse) based on their needs. Taking liver fibrosis staging indicators and values as an example, users can select the mean value "E Mean" of shear wave elastography measurement results within trace box "A" and set four stages "F0", "F2", "F3", and "F4" with corresponding cutoff values of "0 kPa", "6.5 kPa", "8.3 kPa", "10.3 kPa", and "100 kPa". (Note: Multi-parametric grading reference and multi-parametric grading radar chart require the selection of more than three indicators for staging and the number of stages for each indicator must be the same.) Staging indicators and values only need to be entered once, and after completing the settings, the settings can be reused for all subsequent research data.

(a)

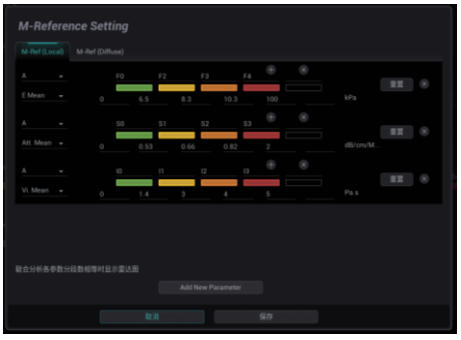

(b)

Figure 9: (a) Before entering M-Ref(Focal) indicators and values; (b) After entering M-Ref(Focal) indicators and values.

After entering the staging indicators and values for M-Ref(Focal) and M-Ref(Diffuse), as shown in Figure 10, the report will display the "Multi-Parametric Grading Reference" and

"Multi-Parametric Grading Radar Chart."

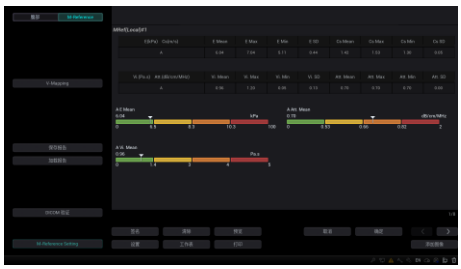

(a)

(b)

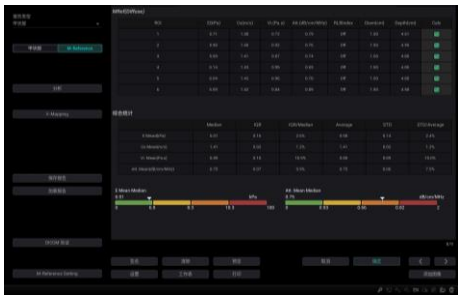

(c)

(d)

Figure 10: (a) M-Ref(Focal) multi-parametric grading reference; (b) M-Ref(Focal) multi-parametric radar chart; (c) M-Ref(Diffuse) multi-parametric grading reference; (d) M-Ref(Diffuse) multi-parametric radar chart

In the "Multi-Parametric Grading Reference" and "Multi-Parametric Grading Radar Chart", different colors represent the severity levels of various parameters, and the markers indicate which severity level each parameter of the current case falls into. Through the "Multi-Parametric Grading Reference" and "Multi-Parametric Grading Radar Chart", the risk levels of multiple parameters in the current case can be visually distinguished, allowing for a more comprehensive evaluation and diagnosis of the current case.

Non-Real-Time Multi-parametric Ultrasound Imaging and Analysis Tool

Real-time multi-parametric ultrasound imaging and analysis cannot be performed on some technologies due to differences and limitations in technical principles. Mindray has proposed a solution of non-real-time multi-parametric ultrasound imaging and analysis for these technologies, such as the M-Ref. C&E multi-parametric ultrasound imaging and analysis function, which enables the simultaneous display and measurement of CEUS and elastography functionalities in the same imaging plane.

M-Ref. C&E

In many studies, sound touch elastography (STE) and sound touch quantification (STQ) technologies have demonstrated excellent sensitivity and specificity in the clinical diagnosis of various diseases by assessing Young's modulus of tissues. However, in practical clinical diagnosis, tissue elasticity is not the only means of detection. Doctors often need to analyze the microcirculation perfusion characteristics of lesions using CEUS imaging to make comprehensive judgments. Different from CEUS imaging at low Mechanical Index (MI), shear wave elastography based on ARF effect is acquired under relative higher MI, which make it difficult to realize real-time

imaging of shear wave elastography and CEUS in the same imaging plane.

Therefore, the Resona platform also provides the M-Ref. C&E function which selects CEUS images, typically CEUS images at peak intensity from a clip image, and automatically matches the tissue image of CEUS with the B-mode image of shear wave elastography in real-time to provide a prompt for the matching degree of the imaging plane. Users can then sequentially obtain CEUS images and shear wave elastography images in the same plane, display them side by side for comparison, and perform synchronized quantitative measurements to obtain information on intensity from CEUS and tissue stiffness from shear wave elastography in the same region. Malignant tumors are often accompanied by changes in tissue stiffness and microcirculation perfusion , shown as “hard rim sign” surrounding tumor in shear wave elastography and high perfusion at early stage and enlarged perfusion range of CEUS. The M-Ref. C&E multi-parametric ultrasound imaging and analysis tool provides an effective tool for observing the changes between the two and guiding related research. Figure 11a, 11b, and 11c show the quad display, dual-window mixed display (MIX), and an example of low similarity case.

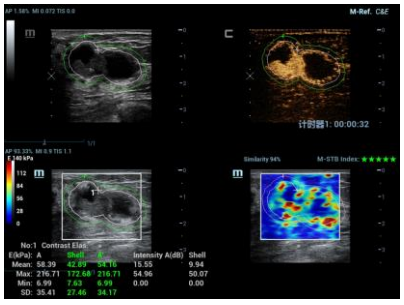

(a)

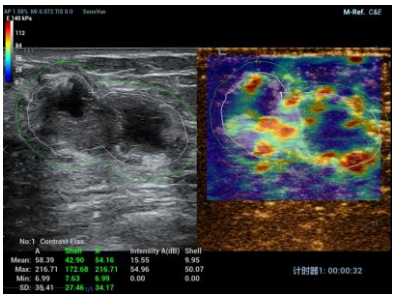

(b)

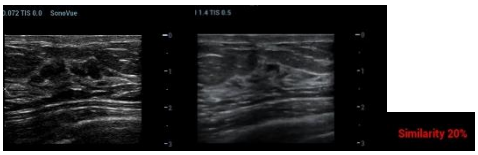

(c)

Figure 11: M-Ref. C&E multi-parametric ultrasound imaging and analysis tool. (a) Quad display; (b) Mixed display; (c) Tissue image of CEUS and B image of shear wave elastography in different image plane results low similarity notification

Case Studies

Application in Breast Diagnosis

The differential diagnosis of benign and malignant breast cancers is one of the most mature and common applications of ultrasound elastography. Both strain elastography and shear wave elastography have demonstrated excellent sensitivity and specificity in the differential diagnosis of breast tumors. Viscoelasticity imaging, as an emerging ultrasound elastography technology related to tissue inflammation, has also shown excellent sensitivity and specificity in the early clinical studies of benign and malignant breast tumors.

Viscoelastography and Shear Wave Elastography Multi-Parametric Ultrasound Imaging and Analysis

In previous clinical researches, doctors used Mindray viscoelastography to conduct clinical studies on more than 400 breast tumor patients, among which the ratio of benign and malignant was close to 1:1. Through the measurement of breast lesions by tracing, the maximum FD of

3 mm shell was used for statistics, and the benign and malignant breast lesions were graded with pathological results as the gold standard. The results show that viscoelastography can effectively distinguish benign and malignant breast lesions, and can supplement the diagnostic results of shear wave elastography.

As shown in Figure 12, there is a significant difference in the measured maximum FD between benign and malignant breast lesions. The mean FD in benign breast lesions is 11.22 m/s/kHz, while in malignant breast lesions, the value reaches 17.35 m/s/kHz.

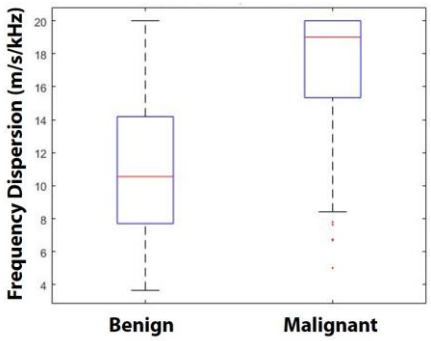

Figure 12: Comparison of FD shell max measurement results for benign and malignant breast lesions

In clinical practice, besides using measurements to quantitatively assess lesion viscoelasticity, qualitative analysis can also be performed based on color maps. In most malignant tumors, the surrounding tissues exhibit high viscosity. Figure 13 shows a typical case of a malignant tumor where the infiltrated surrounding tissue has high viscoelasticity measurements. From the image, it can be seen that the area with high measurements in the viscoelasticity image is larger than the lesion area displayed in the B-mode image.

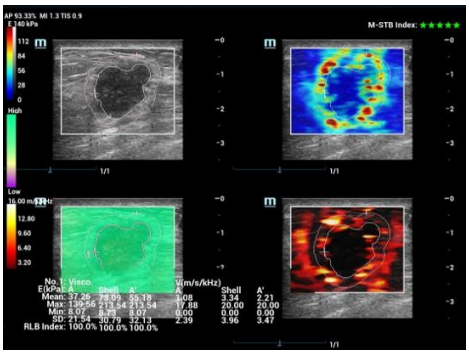

Figure 13: Typical viscoelasticity image of a malignant tumor

Furthermore, in some malignant cases, viscoelastography can provide complementary information to shear wave elastography. Figure 14 shows a case where shear wave elastography measurements are low, while FD measurements are high in a malignant tumor.

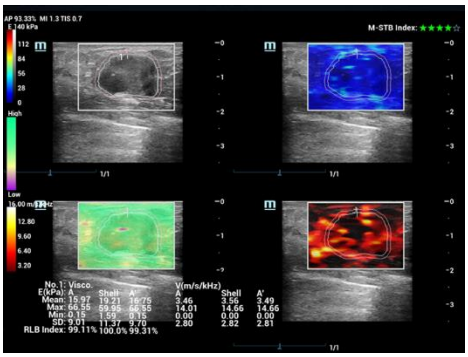

Figure 14: Case of a malignant tumor with low shear wave elastography measurements and high viscoelasticity measurements

M-Ref. E compare Multi-parametric Ultrasound Imaging and Analysis

Studies have shown that the combination and complementarity of strain elastography and shear wave elastography can improve the success rate of benign and malignant differentiation [41-42].

In a well-known hospital in Shanghai, doctors conducted a clinical study on more than 26 breast tumor patients using Mindray's M-Ref. E Compare multi-parametric ultrasound imaging and analysis tool. As shown in Figure

15, the M-Ref. E Compare allowed simultaneous acquisition of strain elastography and shear wave elastography in the same plane of the tumor. Through M-Ref. measurements, quantitative information such as shear wave Young's modulus E (kPa), strain, Young's modulus ratio, and strain ratio were obtained for regions A and B and their corresponding shell regions.

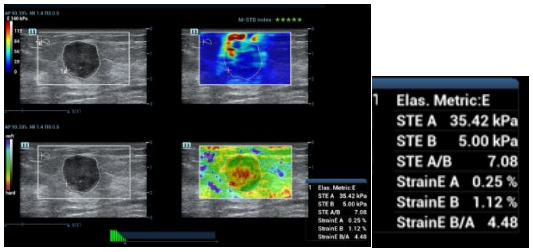

Figure 15: M-Ref. E Compare

The research results showed that by using the strain ratio from strain elastography and the maximum value within the shell region from shear wave elastography for linear regression and generating a benign and malignant diagnosis model, the combination of strain elastography and shear wave elastography using the generated model outperformed the individual use of strain elastography or shear wave elastography alone. As shown in Figure 16, with tissue pathology as the gold standard, the M-Ref. E Compare achieved 0.93 of the area under the receiver operating characteristic curve (AUROC). The AUROC for strain elastography and shear wave elastography as separate evaluation indices were 0.77 and 0.89, respectively.

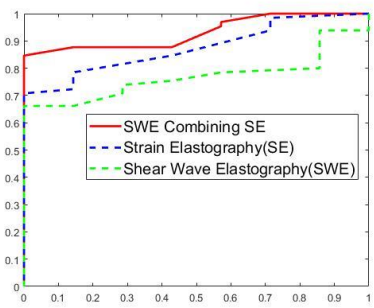

Figure 16: AUROC of M-Ref. E Compare, strain elastography and shear wave elastography.

M-Ref. C&E Multi-parametric Ultrasound Imaging and Analysis

Studies have shown that the combination and complementarity of CEUS imaging and shear wave elastography can improve the success rate of benign and malignant differentiation [43].

In a well-known hospital in Shanghai, doctors conducted a preliminary clinical study on 85 cases of breast tumors using Mindray's M-Ref. C&E multi-parametric ultrasound imaging and analysis tool. During the study, as shown in Figure 17, the shear wave elasticity results of breast lesions was traced according to the lesion area in B-mode imaging as well as in the CEUS imaging. The maximum shear wave elasticity within 2mm shell of lesion area in B-mode imaging and the maximum shear wave elasticity within the lesion area in CEUS imaging are used for statistics respectively. The benign and malignant breast tumors were distinguished with pathological results as the gold standard.

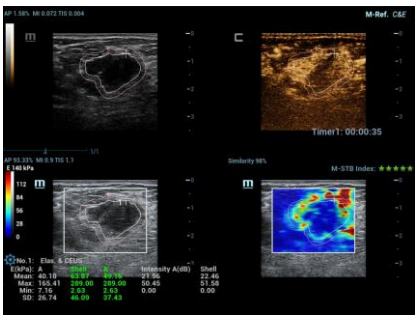

(a)

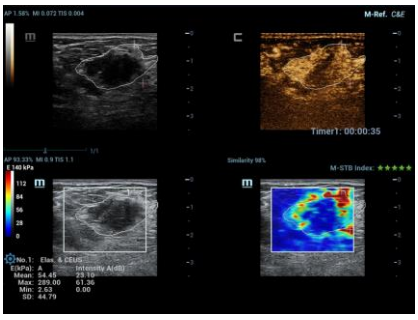

(b)

Figure 17: M-Ref. C&E measurements. (a)

Measurement based on the lesion area displayed in the B-mode image; (b) Measurement based on the lesion area displayed in the CEUS image

As shown in Figure 18, the research results showed that the elastic parameters measured according to the lesion boundary in the CEUS image had a larger AUROC than the elasticity parameters within the shell area traced according to the lesion boundary in the B-mode image, indicating better diagnostic performance.

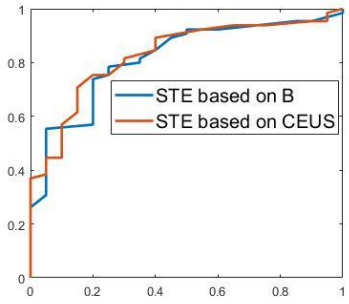

Figure 18: AUROC comparison between elastic parameters measured based on lesion area of B-mode imaging and CEUS imaging

Further research found that for benign and malignant tumor differentiation, the combined analysis of four quantitative parameters from CEUS imaging (AS, DS, PKI, AREA_CEUS) achieved an AUROC of 0.81, shear wave elastography achieved an AUROC of 0.829, while the combination of CEUS quantitative parameters and shear wave elastography quantitative parameters achieved an AUROC of 0.867, as shown in Figure 19.

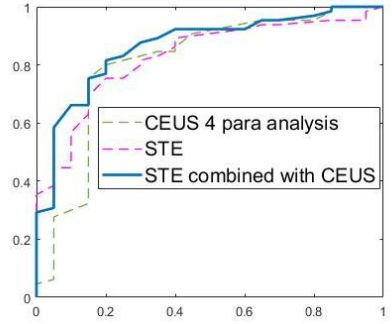

Figure 19: AUROC comparison among combined analysis with CEUS and elastography, CEUS 4-parameter quantitative analysis, and elastography quantitative analysis

Application in Abdominal Diagnosis

The liver is an important organ of the human body. Serious damages of liver function often cause fatal consequences. Most chronic liver diseases often present insidiously, making them easily overlooked and leading to irreversible consequences. Therefore, early detection of liver lesions and monitoring and management of chronic liver diseases are ongoing research focuses in clinical practice. Globally, non-alcoholic fatty liver disease (NAFLD) has replaced viral hepatitis as the leading cause of liver disease, affecting 20%-30% of the global population[44]. In China, the prevalence of NAFLD reached 29.2% (2008-2018).

Due to the complexity and diverse stages of NAFLD, it is challenging to assess the disease using a single parameter. Therefore, Mindray has developed different imaging and quantitative analysis parameters for different liver biomarkers. Attenuation Coefficient (AC) can be used to effectively evaluate fat changes[45-46]. Many clinical studies have shown that STE technology has excellent sensitivity and specificity in the early diagnosis of liver fibrosis and presents good repeatability [15, 47-52]. Viscosity/dispersion is a potential tool for evaluating non-alcoholic steatohepatitis (NASH).

Viscoelasticity and Shear Wave Multi-Parametric Ultrasound Imaging and Analysis

At a renowned liver disease hospital in Shanghai, doctors conducted preliminary clinical research on more than 100 patients using Mindray's viscoelastography. By measuring the liver parenchyma, doctors obtained the mean viscosity coefficient within

a 15 mm circular ROI for statistical analysis. The inflammatory grading of the liver was determined based on pathological results. The research results showed significant differences in the mean viscosity coefficient among different inflammatory grades of the liver, as shown in Figure 20. The mean viscosity coefficient increased with the severity of liver inflammation, and the differences were significant.

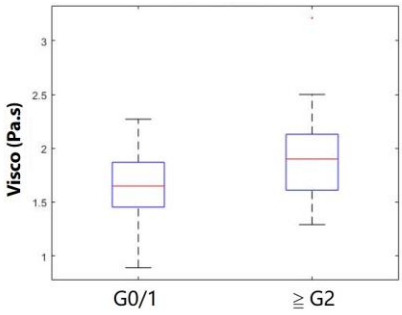

Figure 20: Increase in mean viscosity coefficient with the severity of liver inflammation

It is worth mentioning that in the clinical practice of assessing liver fibrosis using shear wave elastography, it is often found that the measurements tend to be higher when patients have just been admitted and still have inflammation, leading to an overestimation of fibrosis grades when using shear wave elastography alone.

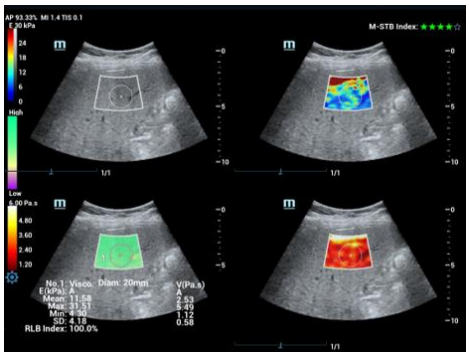

Figure 21: A liver case with elevated shear wave elastography measurement due to inflammation

Figure 21 shows a case which has an inflammation grade of G2 and a fibrosis grade of F1. If the shear wave elastography measurement of 11.58 kPa is used for grading alone, the fibrosis grade would be close to severe fibrosis or cirrhosis. However, considering the influence of inflammation on shear wave elastography measurements, it can be observed that the high shear wave elastography measurement in this case may be due to inflammation. This demonstrates that viscoelasticity has a complementary and corrective effect on shear wave elastography in liver fibrosis diagnosis.

Fatty Liver Multi-Parametric Ultrasound Imaging and Analysis

In a comprehensive liver disease hospital in Guangzhou, doctors conducted a preliminary clinical study on 78 patients using Mindray's USAT technology. They measured the USAT in the liver parenchyma by taking the average value within a 20x20 mm rectangular measurement box and classified the degree of liver fat based on the reference standard of Magnetic Resonance Imaging Proton Density Fat Fraction (MRI-PDFF). As shown in Figure 22, the research results showed significant differences in the USAT values among cases with different degrees of fatty liver. As shown in Table1, USAT showed good sensitivity and specificity in steatosis diagnosis.

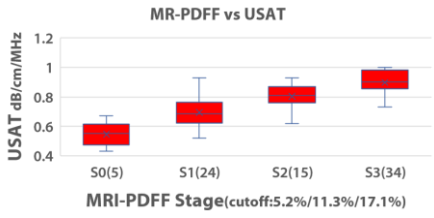

Figure 22: Significant differences in USAT among cases with different degrees of fatty liver

Table1: Diagnostic performance and optimal cutoffs of USAT using MRI-PDFF as the reference standard

Grade	AUC	Cutoff	Sensitivity	Specificity

		(dB/cm/MHz)	(%)	(%)
>S0	0.960	0.67	83.56	100
>S1	0.917	0.75	89.80	79.31
>S2	0.890	0.81	82.35	81.82

In the latest clinical application research on fatty liver, multi-parametric ultrasound imaging and analysis has shown its value in providing multidimensional diagnostic information and quantitative assessment indicators compared to traditional single ultrasound imaging, enabling comprehensive evaluation and precise quantification.

In previous studies, the multi-center results of liver shear wave elastography showed that using 6.5 kPa and 10.3 kPa as cutoff values can serve as reference standards for grading chronic hepatitis B liver fibrosis (F0-F1, F2-F3, F4). In a preliminary clinical experiment involving more than 30 cases, viscoelasticity measurements using 1.4 Pa.s as a cutoff value effectively distinguished the presence of hepatitis. In a preliminary clinical study of fatty liver grading involving over 300 cases, cutoff values of 0.53, 0.66, and 0.82 dB/cm/MHz achieved effective differentiation of S0, S1, S2, and S3 grades of fatty liver lesions.

In a case study of a normal individual without liver fibrosis, fatty liver, or hepatitis, as shown in Figure 23a, the liver shear wave elastography measurement was 4.55 kPa, the viscosity measurement was 0.94 Pa.s, and the USAT measurement was 0.48 dB/cm/MHz, all within the normal range.

In a case study of hepatitis B virus-related cirrhosis without fatty liver, as shown in Figure 23b, the liver shear wave elastography measurement was 15.91 kPa, the viscosity measurement was 1.6 Pa.s, and the USAT measurement was 0.42 dB/cm/MHz. The USAT measurement was within the normal range, while the shear wave elastography measurements were significantly higher than the normal range. The viscosity measurements were slightly higher than the normal range, which might be relative to inflammation.

In a case study of a non-fibrosis fatty liver, as shown in Figure 23c, the liver shear wave elastography measurement was 6.3 kPa, the viscosity measurement was 0.74 Pa.s, and the USAT measurement was 0.74 dB/cm/MHz. Both the shear wave elastography and viscoelasticity measurements were within the normal range, but the USAT measurement was significantly higher than the normal range, indicating purely fatty liver excluding NASH.

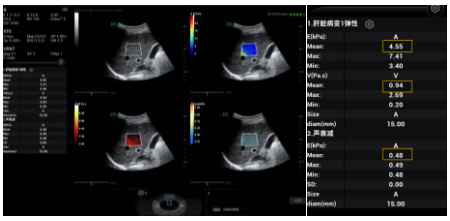
(a)

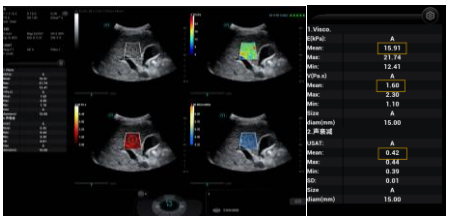
(b)

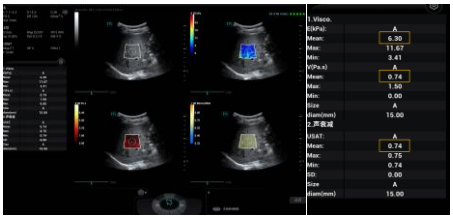
(c)

Figure 23: (a) Multi-parametric measurements of a normal liver; (b) Multi-parametric measurements of a liver with cirrhosis and hepatitis without fatty liver; (c) Multi-parametric measurements of NASH case.

Conclusion

Mindray's M-Ref technology provides a solution for multi-parametric ultrasound diagnosis. By combining real-time or non-real-time analysis, it enables a comprehensive evaluation of tissue and lesions from various perspectives, including mechanical parameters, acoustic parameters, morphological parameters, and blood perfusion parameters. The "multi-parametric grading reference" and "multi-parametric grading radar chart" assist doctors in making comprehensive and intuitive judgments about the risk of lesions. Currently, Mindray's multi-parametric ultrasound imaging and analysis tool is mainly applied in liver, breast, and thyroid examination. In the future, it is expected to be applied in more field such as prostate, gynecology, and musculoskeletal, and provide more accurate and detailed clinical diagnostic reference indicators to better assist clinical diagnosis.

References

[1] Rubini A, Guiban O, Cantisani V, et al. Multiparametric ultrasound evaluation of parotid gland tumors: B-mode and color Doppler in comparison and in combination with contrast-enhanced ultrasound and elastography. A case report of misleading diagnosis. J Ultrasound 2021; 24(3)

[2] Basavarajappa L, Baek J, Reddy S, et al. Multiparametric ultrasound imaging for the assessment of normal versus steatotic livers. Sci Rep 2021; 11(1)

[3] Kapetas P, Clauser P, Woitek R, et al. Quantitative Multiparametric Breast Ultrasound: Application of Contrast-Enhanced Ultrasound and Elastography Leads to an Improved Differentiation of Benign and Malignant Lesions. Invest Radiol 2019; 54(5)

[4] Gao J, Lee R, Trujillo M, et al. Reliability of Performing Multiparametric Ultrasound in Adult Livers. J Ultrasound Med 2022; 41(3)

[5] Tang A, Destrempes F, Kazemirad S, et al. Quantitative ultrasound and machince learning for assessment of steatohepatitis in a rat model. European Radiology 2019; 29:2175-2184

[6] Giovanna F, et al. Liver ultrasound elastography: an update to the world federation for ultrasound in medicine and biology guidelines and recommendations. Ultrasound in Med & Biol, 2018; 00(00):1-22

[7] Richard G.B, Stephanie R.W, Deborah R, et al. Update to the society of Radiologists in ultrasound liver elastography consensus statement. Radiology, 2020; 00:1-12

[8] Chinese Society of Hepatology, Chinese Medical Association, et al. Consensus on the diagnosis and therapy of hepatic fibrosis. Clin Hepatol,2019;35(10):2163-2172

[9] Anke Thomas. Real-time sonoelastography performed in addition to B-mode ultrasound and mammography: improved differentiation of breast lesions? Academic Radiology. 2006;13(12):1496-1504

[10] Richard G.B. Breast Elastography: How to perform and integrate into a "Best-Practice" patient treatment algorithm. J Ultrasound Med. 2020; 39:7-17

[11] Lei Z, Zhimin D, Fajin D, et al. Diagnostic performance of multiple sound touch elastography for differentiating benign and malignant thyroid nodules. Front. Pharmacol. 9:1359

[12] Anke Thomas. ReaL-time sonoelastography of the cervix: tissue elasticity of the normal and abnormal cervix. Academic Radiology. 2007;14(2):193-200

[13] Jianqiao Zhou, Weiwei Zhan, et al. Stiffness of the surrounding tissue of breast lesions evaluated by ultrasound elastography. European Society of Radiology. 2014; DOI 10.1007/s00330-014-3152-7

[14] Lu-ying G, Yang G, Wen X, et al. Can combined screening of ultrasound and elastography improve breast cancer identification compared

with MRI in women with dense breasts-a multicenter prospective study. 2020; 11(13):3903-3909

[15] Jinfen W, Manli W, et al. Usefulness of new shear wave elastography technique for noninvasive assessment of liverfibrosis in patients with chronic hepatitis B: a prospective multicenter study. Ultraschall in Med. 2021

[16] Leah A.G, Andrew T.T, Paula B, et al. Repeatability and agreement of shear wave speed measurements in phantoms and human livers across 6 ultrasound 2-dimensional shear wave elastography systems. Invest Radiol, 2020;55(4):191-199

[17] Xiao L, Hong-kui Y, Shu-ya S, et al. Quantitative evaluation of passive muscle stiffness by shear wave elastography in healthy individuals of different ages. European Radiology. 2020;31(5):3187-3194

[18] Bertrand G, et al. In vivo assessment of the levator ani muscles using shear wave elastography: a feasibility study in women. Int Urogynecol J. 2019;30(7):1179-1186

[19] Jimei S, Nan L, Wei J, et al. Clinical application of cervical shear wave elastography in predicting the risk of preterm delivery in DCDA twin pregnancy. BMC Pregnancy and Childbirth. 2022; 22:202

[20] Ruobing H, Zehui L, et al. AW3M: An auto-weighting and recovery framework for breast cancer diagnosis using multi-modal ultrasound. Med Image Anal. 2021;72:102137

[21] Gian Piero B, el al. "lasto-lung point": A new tool for the sonographic confirmation of pneumothorax. Clin Respir J. 2020;14(8):758-762

[22] Thineskrishna A, Cheng W, et al. Characterisation of prostate lesions using transrectal shear wave elastography(SWE) ultrasound imaging: a systematic review. Cancers 2021;13:122

[23] Lana B.H.Keijzer, Mihai S, et al. Reproducibility of natural shear wave elastography measurements. Ultrasound in Med. &Biol. 2019;45(12):3172-3185

[24] Sugimoto K, Moriyasu F, Oshiro H, et al. Viscoelasticity Measurement in Rat Livers Using Shear-Wave US Elastography. Ultrasound Med Biol. 2018;44(9):2018-2024.

[25] Sugimoto K, Moriyasu F, Oshiro H, et al. The Role of Multiparametric US of the Liver for the Evaluation of Nonalcoholic Steatohepatitis. Radiology. 2020;296(3):532-540.

[26] Kumar V, Denis M, Gregory A, Bayat M, et al. Viscoelastic parameters as discriminators of breast masses: Initial human study results. PLoS One. 2018;13(10):e0205717.

[27] Ferraioli G, et al. Ultrasound-based techniques for the diagnosis of liver steatosis. World J Gastroenterol. 2019; 25(40):6053-6062

[28] Wan CF, Du J, Fang H, et al. Enhancement Patterns and Parameters of Breast Cancers at Contrast-enhanced US: Correlation with Prognostic Factors. Radiology 2012; 262(2)

[29] Boca, I, Dudeam S.M, Ciurea A.I. Contrast-Enhanced Ultrasonography in the diagnosis and Treatment Modulation of Breast Cancer. J.Pers.Med. 2021, 11, 81

[30] Sarvazyan AP, Rudenko OV, Swanson SD, Fowlkes JB, EmelianovSY. Shear wave elasticity imaging: A new ultrasonic technology of medical diagnostic. Ultr. Med Biol 1998;20:1419 –1436.

[31] M. L Palmeri., M. H Wang. Quantifying hepatic shear modulus in vivo using acoustic radiation force. Ultrasound in Med & Biol. 2008;34(4):546-558

[32] Joyce McLaughlin and Daniel Renzi. Shear wave speed recovery in transient elastography and supersonic imaging using propagating front. Inverse Problems.2006; 22:681–706

[33] JLGennisson, SCatheline, et al. Transient elastography in anisotropic medium: Application to the measurement of slow and fast shearwave speeds in muscles. J Acoustical Society of America. 2003;114:536-541

[34] M. L Palmeri., M. H Wang. Quantifying hepatic shear modulus in vivo using acoustic radiation force. Ultrasound in Med & Biol.

2008;34(4):546-558

[35] G R Torr. The acoustic radiation force. Am. J. Phys. 1984; 52(5)

[36] Catheline S, Gennisson JL, Delon G, et al. Measuring of viscoelastic properties of homogeneous soft solid using transient elastography: an inverse problem approach. J Acoust Soc Am. 2004;116(6):3734-41.

[37] Xinping Ren, Shujun Xia, Lu Zhang, et al. Analysis of liver steatosis analysis and controlled attenuation parameter for grading liver steatosis in patients with chronic hepatitis B. Quant Imaging Med Surg. 2020.

[38] Ferraioli G, et al. Quantification of Liver Fat Content with Ultrasound: A WFUMB Position Paper. Ultrasound Med Biol. 2021 Oct;47(10):2803-2820.

[39] Napolitano D, Chou CH, McLaughlin G, et al. Sound speed correction in ultrasound imaging. Ultrasonics 2006; 44 e43-e46

[40] Wanger RF, Smith SW, Sandrik JM, et al. Statistics of Speckle in Ultrasound B-Scans. IEEE Transactions on Sonics and Ultrasonics 1983; 30(3)

[41] Huang S, Ye X, Yang K, et al. The significance of dual-mode elastography in the diagnosis of breast lesions by physicians with different levels of experience. Quant Imaging Med Surg. 2022 Feb; 12(2)

[42] Seo M, Ahn HS, Park SH, et al. Comparison and combination of strain and shear wave elastography of breast masses for differentiation of benign and malignant lesions by quantitative assessment: Preliminary Study. J Ultrasound Med. 2018 Jan; 37(1): 99-109

[43] He H, Wu X, Jiang M, et al. Diagnostic accuracy of contrast-enhanced ultrasound synchronized with shear wave elastography in the differential diagnosis of benign and malignant breast lesions: a diagnostic test. Gland Surg 2023; 12(1):54-66

[44] Zhou J, Sun HC, wang, Z, et a1. Guidelines for diagnosis and treatment of primary liver cancer in China (2017 edition) [J]. Liver Cancer. 2018, 7(3): 235—260.

[45] Meijuan Jiang, Xuanxuan Zhang, Xiaojin Wu, et al. The diagnostic value of novel ultrasound attenuation analysis in detecting liver steatosis identified by the controlled attenuation parameter: a diagnostic accuracy study. Ann Transl Med 2023.

[46] E.M.Jung, Yi Dong, F. Jung. Current aspects of multimodal ultrasound liver diagnostics using contrast-enhanced ultrasonography (CEUS), fat evaluation, fibrosis assessment, and perfusion analysis – An update.

[47] Ilias G, Petros D, Spyros Y, et al. Comparison of sound touch elastography, shear wave elastography and vibration-controlled transient elastography in chronic liver disease assessment using liver biopsy as the "eference Standard". Ultrasound Med & Biol. 2020;46(4):959-971

[48] Lulu Y, Jiawu L, Lin M, et al. Noninvasive assessment of liver fibrosis in chronic hepatitis B carriers with sound touch elastography: study of surgical pathology specimens. Expert Rev Med Devices. 2020;17(8):845-853

[49] Lulu Y, Wenwu L, Du H, et al. Shear wave-based sound touch elastography in liver fibrosis assessment for patients with autoimmune liver diseases. Quant Imaging Med Surg. 2021;11(4):1532-1542

[50] Xinping Ren, Shujun Xia, Zhongxin Ni, et al. Analysis of three ultrasound elastography techniques for grading liver fibrosis in patients with chronic hepatitis B. Radiol Med. 2018;123(10):735-741

[51] Ruo-kun Li, Xin-pin Ren, Fu-hua Yan, et al. Liver fibrosis detection and staging: a comparative study of T1p MR imaging and 2D real-time shear-wave elastography. Abdom Radiol(NY). 2018;43(7):1713-1722

[52] Kun Huang, Qinyuan Li, Weimei Zeng, et al. Ultrasound score combined with liver stiffness measurement by sound touch elastography for staging liver fibrosis in patients with chronic hepatitis B: a clinical prospective study. Ann Transl Med. 2022;10(6):271

mindray

healthcare within reach